

HYDROTHERMAL SYNTHESIS OF METAL OXIDE NANOPARTICLES

V.I. Anikeev

Boreskov Institute of Catalysis SB RAS, prosp. Lavrentieva 5,
Novosibirsk 630090, Russian Federation

E-mail: anik@catalysis.nsk.su

ABSTRACT

Continuous hydrothermal synthesis of metal oxide nano- and microparticles in supercritical water was performed in a continuous flow reactor. The results of investigation of LiCoO₂, LiNiO₂, LiZnO₂, LiCuO₂, Ga₂O₃, CeO₂ nanoparticles by HRTEM and XRD analysis were presented.

INTRODUCTION

Metal and metal oxide nanoparticles, differing from their bulk analogs in chemical, thermal, optical, magnetic and other properties, are widely used in catalysis, medicine, electronics and other fields. The field of nanoparticles application depends not only on their properties (size, structure and morphology), but also on the method of their synthesis. Nanoscale of the material is determined by one of its dimensions (diameter or thickness) varying in the range of 1 to 200 nm.

Nanoparticles of metals and/or their oxides supported on various surfaces are of special interest due to their unique features related with morphology, dispersity and surface concentration of a metal. Thus, nanoparticles with high specific surface area supported on various substrates are used as catalysts for numerous chemical transformations.

Many different methods of nanoparticle synthesis with the use of supercritical fluids (SCF) have been suggested, in particular, the reverse micelle, rapid expansion and hydrothermal synthesis methods [1-4].

Among the main problems of all synthesis methods, both suggested and in use, is their flexibility in controlling the size, concentration and distribution of synthesized nanoparticles. The use of SCF as a medium for nanoparticles synthesis provides numerous advantages caused by special features of SCF. Some properties of substances in supercritical state differ from those of liquid or gas and are highly sensitive to minor changes in temperature or pressure. For instance, heat capacity, viscosity and density of a substance change considerably near the critical point. Since density of *cs*-fluid may be equal or exceed the density of liquid, *cs*-fluids are good solvents for many organic compounds.

In contrast to common liquids, *cs*-fluids provide high diffusivity and have low viscosity, which lead to intensification of heat- and mass-transfer processes. Low surface tension of *cs*-fluids allows reactants to penetrate easily into the pores due to better wetting of the surface in comparison with liquids.

Continuous hydrothermal synthesis in supercritical water (SCW) has the best advantages and possibilities among the methods suggested for synthesis of metal and metal oxide nanoparticles [5-9]. This method is simple to implement and scale up, it allows controlling the particles size and properties. However, an essential drawback of the method consists in low control of nanoparticles aggregation.

The present study is devoted to hydrothermal synthesis of metal oxide nanoparticles with the use of SCW.

EXPERIMENTAL SETUP AND PROCEDURE

Figure 1 shows a schematic of the setup used for nanoparticles synthesis by hydrothermal method. The setup includes a tubular reactor consisting of two parts, each 3 m in length with inner diameter 1.75 mm (in this case, the reactor capacity is 7.2 or 14.4 cm³). There are also two piston pumps, syringe pump, back pressure valve, electric furnace with fluidized sand bed, cooler, flow mixer, manometers and pressure gauges.

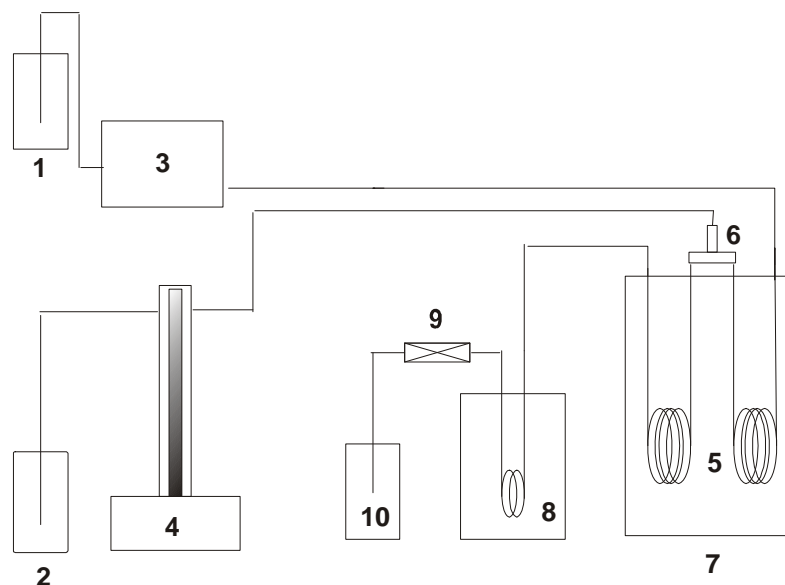


Figure 1. Setup for nanoparticles synthesis by hydrothermal method. 1, 2- volumes to water and reagents; 3 – piston pump; 4 – syringe pump; 5 – tubular reactor; 6 – mixer; 7 – oven with fluidized sand bed; 8 – cooler; 9 – back pressure regulator; 10 – volume for the products

All syntheses of metal oxides were carried out virtually by the same procedure: the initial parent solution for synthesis of the above listed compounds was prepared by dissolution in water of equimolar or different molar amounts of nitrate, sulfate or acetate of the first metal, M_1 , with other salt of the second metal, M_2 . The parent solution was introduced by a syringe pump into mixer 9 in a 1:10 ratio to supercritical water, which was introduced into the same mixer by a piston pump in a continuous mode. Transformations were performed at temperatures and pressures close to critical parameters of the mixture containing more than 95% of water: temperature above 371°C and pressure exceeding 230 atm. Products of the salt – SCF interaction went from reactor to heat exchanger, through back pressure valve to collecting vessel.

RESULTS AND DISCUSSION

Hydrothermal syntheses of LiM_xO_y metal oxide nanoparticles

Hydrothermal synthesis of expected metal oxide compounds LiCoO_2 , LiNiO_2 , LiZnO_2 and LiCuO_2 , one of which is Li, was performed under continuous mode in a flow type reactor. LiMO_x compounds were synthesized in supercritical water mainly by the same procedure.

The initial parent solutions for synthesis of the above listed compounds were prepared by dissolution of two salts in water:

LiCoO_2 : 0.1 M lithium nitrate LiNO_3 + 0.1M cobalt sulfate CoSO_4

LiNiO_2 : 0.1 M lithium nitrate LiNO_3 + 0.1M nickel acetate $\text{Ni}(\text{CH}_3\text{COO})_2$

LiZnO_2 : 0.1 M lithium nitrate LiNO_3 + 0.1M zinc sulfate ZnSO_4

LiCuO_2 : 0.1 M lithium nitrate LiNO_3 + 0.1M copper acetate $\text{Cu}(\text{CH}_3\text{COO})_2$

The parent solution was fed to reactor – flow 2 via mixer, where it was mixed with supercritical water – flow 1.

LiCoO_x synthesis

The temperature of hydrothermal synthesis varied from 382 to 387°C at pressure 226-230 atm. Flow 1 – 10 ml/min, flow 2 – 2 ml/min.

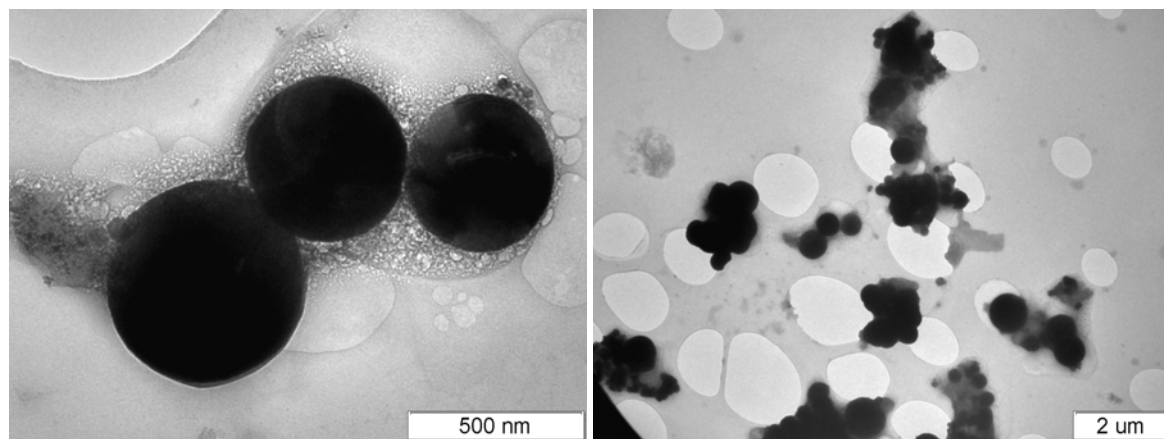


Figure 2 a, b. HRTEM images of the synthesized compound

Figures 2 a, b show HRTEM images of nanoparticle products of hydrothermal synthesis. LiCoO_x particles have spherical shape and size 500 nm. These particles are surrounded with a coat consisting of the products that formed after drying of the solvent. Coarse particles of size ~500 nm form agglomerates of 3–4 particles, smaller particles of size less than 500 nm form agglomerates of 10 and more particles.

LiNiO₂ synthesis

Figures 3 a, b show the HRTEM images of a synthesized sample of the target compound, which looks like sandwich plates with size ~ 50 nm and thickness $\sim 2-3$ nm. For this structure, atomic spacing of the planes corresponds to LiNiO₂. However, the sample has also more contrast particles of size 3-5 nm, for which parameter 0.246 nm was determined, similar to the sandwich phase. This gives ground to conclude that the sandwich phase is LiNiO₂ (high substitution of lithium for nickel), whereas small contrast particles have low substitution and correspond to the NiO phase. The latter is confirmed by XRD data.

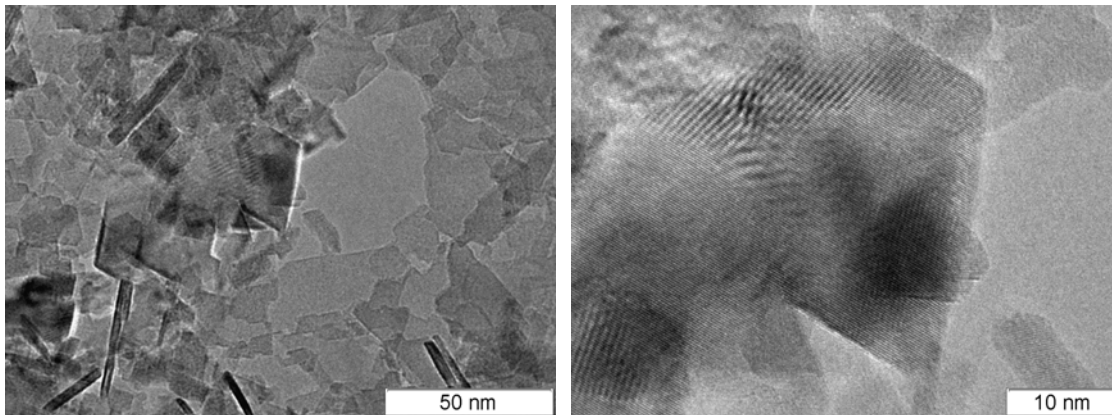


Figure 3 a, b. HRTEM images of the samples of LiNiO₂ compound

LiZnO₂ synthesis

Figure. 4 shows HRTEM image of a synthesized sample of the target compound. One can see that the synthesis product is represented by two-type structures: plates (typical size: ~ 10 nm \times ~ 1 μ m) and aggregates of isometric crystals with size not exceeding 10 nm. Plates are unstable under the HRTEM electron beam: structure disordering occurs. EDX gives an intense Zn line for plates.

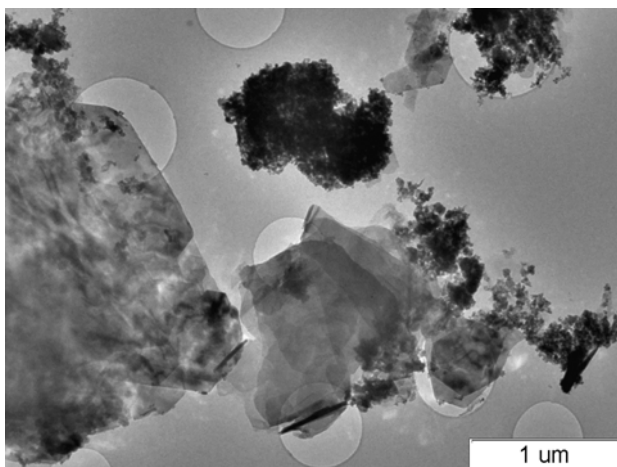


Figure 4. HRTEM image of a sample of LiZnO₂ compound

LiCuO_x synthesis

The synthesized sample is a polycrystalline mixture of crystals with high degree of cutting corresponding to cubic symmetry and quite uniform in habit, Fig. 5 a, b. Their shape and size: isomorphous (cubes) ≈ 50 nm, elongate (parallelepipeds) $\approx 50 \times 150$ nm, flat (plates) 50×100 nm. Dendrite aggregates of these crystals prevail. On the crystal surface under the TEM electron beam, an amorphous molecular layer of molecular thickness is formed, which is typical of lithium crystalline compounds.

The calculated interatomic plane distances (0.282; 0.257; 0.232; 0.1894 av.; 0.1668; 0.1508; 0.1388 av.) correspond to lithium cuprite and CuO. XRD data confirm CuO.

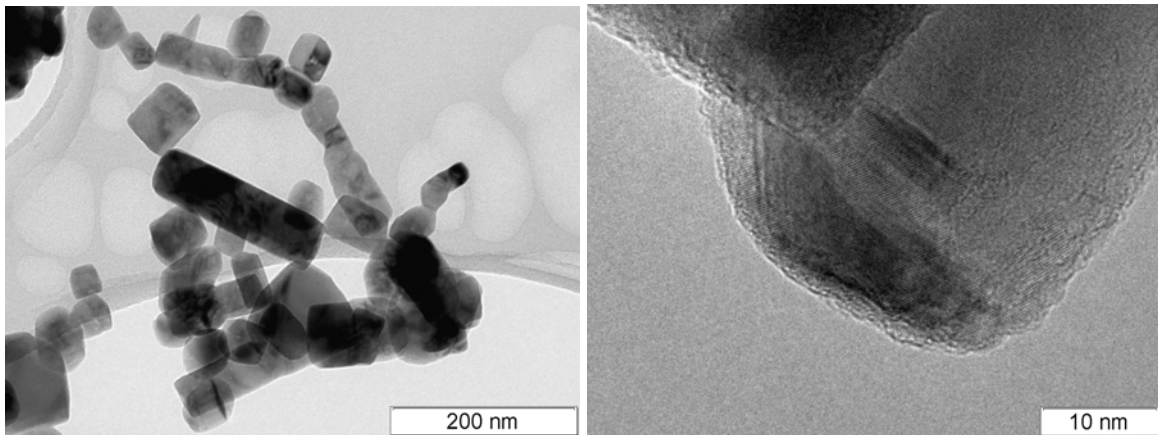


Figure 5 a,b. HRTEM images of LiCuO₂ compound

EDX gives an intense Cu line with weak lines from admixtures.

Hydrothermal syntheses of M_yO_x metal oxide nanoparticles

Hydrothermal synthesis of metal oxides Ga_yO_x, Ce_yO_x was performed under continuous mode in a flow type reactor. All syntheses of M_yO_x compounds in supercritical water were carried out by the same procedure.

Ga₂O₃ synthesis

To synthesize the target compound, a 0.1 M water solution of Ga(NO₃)₃ 8H₂O salt was prepared. The process temperature was 365-384°C, pressure 235 atm. Water flow rate: flow 1 – 10 ml/min, reactant flow rate: flow 2 – 2 ml/min. The reaction products were represented by a dark homogeneous solution.

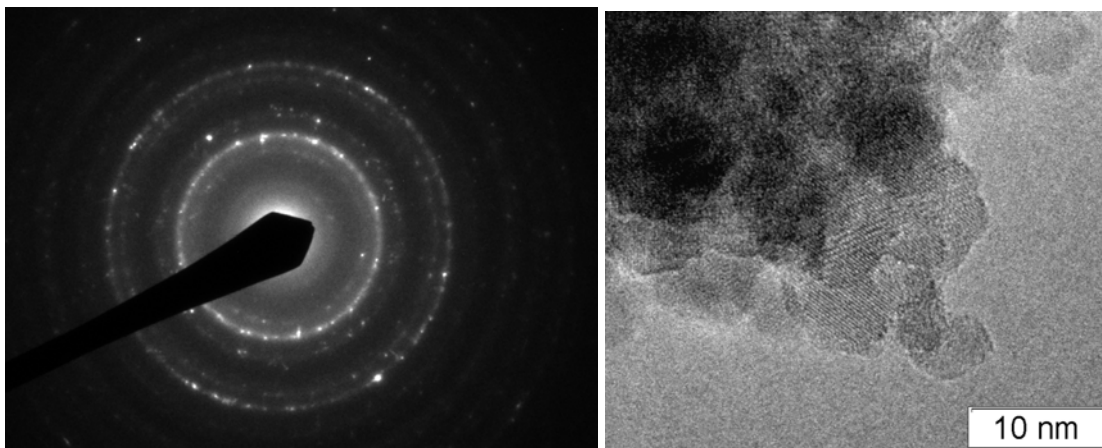


Figure 6 a,b. HRTEM images of Ga_2O_3 compound

The synthesized compound was represented by crystals with high dispersity, 2-5 nm, Fig. b. Isolated blocks of pseudomorphous crystals are present (size of pseudomorphous crystals — up to 100 nm). EDX gives an intense Ga line.

XRD analysis showed that the main phase of synthesized compound was $\gamma\text{-Ga}_2\text{O}_3$ in combination with unidentified crystal phase.

CeO_2 synthesis

A 0.2 M water solution of $\text{Ce}(\text{NO}_3)_3$ salt was prepared for the synthesis. The reaction temperature was 373-391°C, pressure 260 atm. Water flow rate: flow 1 – 10 ml/min, reactant flow rate: flow 2 – 3 ml/min. The reaction products of whitish yellow color, with further precipitation of the solid phase.

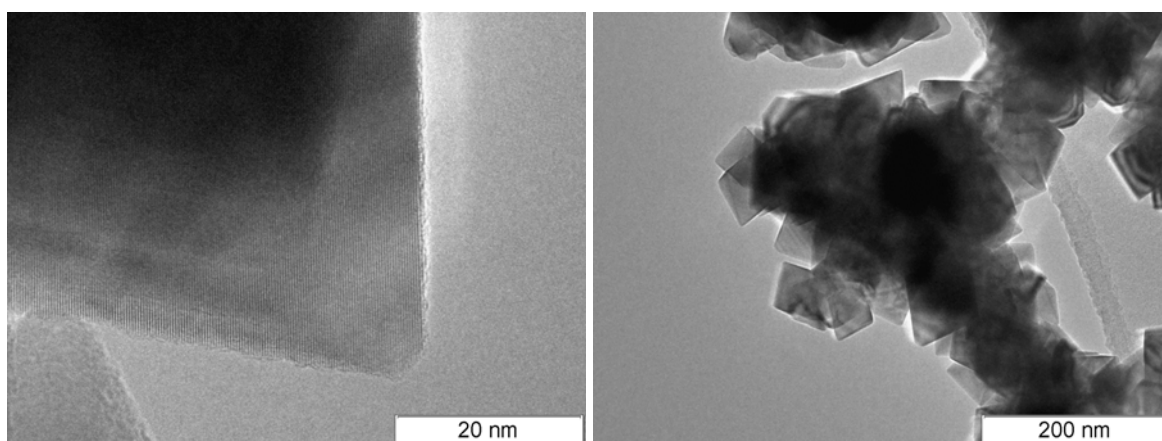


Figure 7 a, b. HRTEM images of CeO_2 compound

Solid products of the synthesis were represented by a homogeneous mixture of well-cut isometric crystals ~ 100 nm in size, Fig. 7 a, b. Dendrite aggregates of these crystals prevail.

The crystals are of dislocation block structure. EDX gives an intense Ce line. According to XRD data, CeO₂ is the main synthesized phase.

REFERENCES

- [1]. Reverchon E., Adami R., J. of Supercritical Fluids, Vol. 37, **2006**, p.1.
- [2]. Jung J., Perrut M., J. of Supercritical Fluids, Vol. 20, **2001**, p.179.
- [3]. Zhang Y., Erkey C., J. of Supercritical Fluids, Vol. 38, **2006**, p. 252.
- [4]. Aymonier C., Loppiner-Serani A., Reveron H., Garrabos Y., Cansell F., J. of Supercritical Fluids, Vol. 38, **2006**, p. 242.
- [5]. Adschiri T., Hakuta Y., Arai K., Ind. Eng. Chem. Res., Vol. 39, **2000**, p. 4901.
- [6]. Adschiri T., Hakuta Y., Sue K., Arai K., J. Nanopart. Res., Vol. 3, **2001**, p. 227.
- [7]. Cabanas A., Darr J., Lester E., Poliakoff M., J. Mater. Chem., Vol. 11, **2001**, p. 561.
- [8]. Adschiri T., Takami S., Umetsu M., Ohara S., Ceram. Trans., Vol. 146, **2005**, p. 3.
- [9]. Kawasa S., Xiuyi Y., Sue K., Hakuta Y., Suzuki A., Arai K., J. of Supercritical Fluids, Vol. 50, **2009**, p. 276.